Appl. Phys. B 37, 73–78 (1985)

Applied Physics B Photophysics and Laser Chemistry

Inversion of Atomic Resonance Transitions by Electron Collisional Dissociation

M. Neiger, W. Kaesler*, and H.-P. Popp

Lichttechnisches Institut, University, D-7500 Karlsruhe, Fed. Rep. Germany

Received 19 November 1984/Accepted 28 January 1985

Abstract. Population inversion of several resonance transitions in the rare-earth atom thulium has been achieved by electron collisional dissociation of TmI_3 molecules in a fast electric discharge configuration. The inversion manifests itself by a strong spiking behavior during the initial current rise and lasts for several nanoseconds. Results of a model calculation of this inversion process for resonance lines support our experimental findings.

PACS: 42.55, 42.60, 51.70

Incoherent resonance line lamps are used widely for the detection of trace metal-atom concentrations [1]. For remote sensing applications laser sources with their vastly superior brightness are necessary, such as, for example, dye lasers. However, the technology required to obtain even low-power frequency-locked dye-laser radiation seems complex and cumbersome for many applications [1]. Optically pumped resonance line lasers, as developed during the past few years [2–4], are a considerably simpler alternative. Due to the nature of resonance lines with the lower level of the transition being the atomic ground state, the pumping process for population inversion must start from a suitable molecular species and selectively populate the resonance level via a dissociation process. Photodissociation has been used in the above-mentioned case of optically pumped resonance lasers. However, such lasers require excimer lasers or frequency multiplied Nd:YAG lasers as pump sources, because pumping has to take place within a few tens of nanoseconds to be able to compete with resonance fluorescence of the upper laser level.

It is the purpose of our work to study the possibility of creating the desired resonance line inversion by selective electron impact dissociation in a fast, diffuse electrical glow discharge. Electron impact dissociation in such discharges has been used before for pulsed gas discharge lasers, e.g. $HgBr_2$ lasers [5], or CdI_2 lasers [6]. To our knowledge, however, such electrically driven resonance line inversion has not been achieved yet.

Experiment

In our experiments we investigated resonance lines of the rare-earth atom thulium (Tm). The reason for this choice is the existence of a multitude of resonance lines of Tm with moderate oscillator strengths and within a relatively small spectral range in the blue and near uv region. This is due to the rich level structure of this rare-earth element with a still simple dublett splitted ground state [7]. As a suitable molecular species we selected thuliumtriiodide (TmI_3), which can be vaporized with sufficient partial pressure at still reasonable temperatures [8].

Fast electrical discharge experiments in mixtures of Ar and TmI_3 vapors have been performed. As the pumping process has to compete with resonance fluorescence, a very fast discharge current rise in the 10 ns range is required.

Figure 1 shows a schematic of the low-inductance discharge circuit used, which yields current rise times of the order of 30 ns. The capacitors used were in the range 0.2–8 nF ($BaTiO_3$) with discharge voltages between 6 and 20 kV. A low-induction hydrogen

* Present address: Laboratorium für Mikrowellenanwendungen, (Dr. Beerwald), D-4630 Bochum, Fed. Rep. Germany

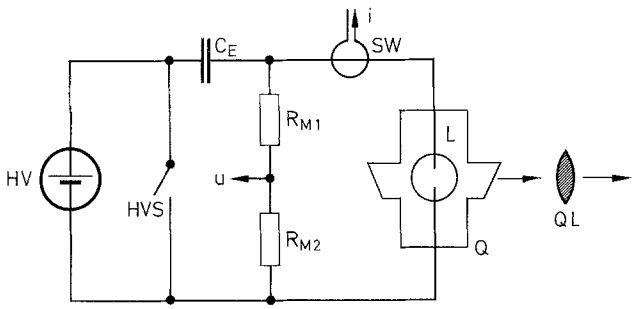

Fig. 1. Schematic of the low-inductance discharge circuit and observation geometry. (HV: high voltage supply, HVS: thyratron switch HY 1102, CE: discharge capacitor, RM: high voltage divider, SW: current transformer meter, L: lamp housing, Q: quartz oven, QL: quartz lens)

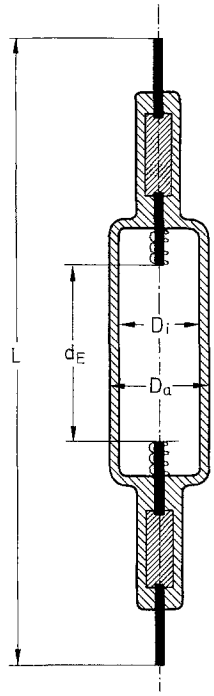

Fig. 2. Schematic of the discharge tube. (outer diameter: 18–22 mm, inner diameter: 15–18 mm, electrode separation: 20–35 mm, overall length: 120 mm, overall volume: 7 ccm)

thyratron (HY 1102) initiates the discharge pulses, which can be repeated at a rate of up to 30 pps.

Figure 2 shows an example of the type of discharge vessel used in our experiments. The tubes are made of water-free quartz and connected to the discharge circuit in an approximately coaxial manner. They are filled with argon gas (10–100 mb pressure) and an excess amount of solid TmI_3. The discharge is operated in an oven in the temperature range 300–1200 K, i.e. at TmI_3-vapor pressures up at 10 mb. A heated side-on window permits spectroscopic observation of the discharge pulses with a high spectral resolution (0.003 nm) grating monochromator.

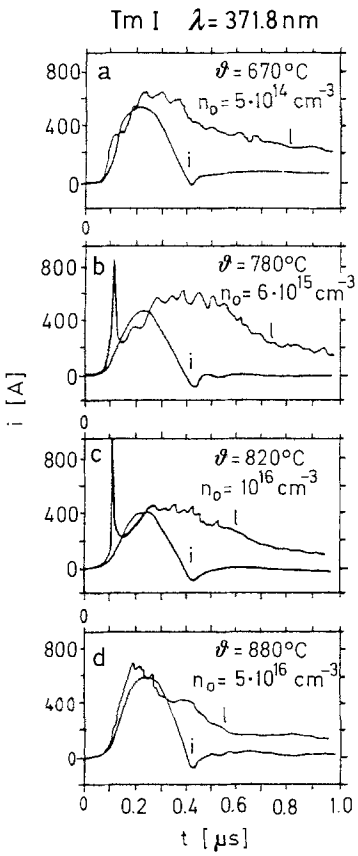

Fig. 3. Oscillograms of discharge current $i(t)$ and resonance line signal $I(t)$ of Tm I $\lambda = 371.8$ nm for 4 different oven temperatures (TmI_3 vapor pressures) with the following discharge parameters: $U_C = 10$ kV, $C_E = 6.6$ nF, $p_{Ar} = 40$ mb

Figure 3 shows oscillograms of the discharge current $i(t)$ and the photomultiplier signal $I(t)$ of the Tm resonance line $\lambda = 371.8$ nm versus time after initiation of the discharge pulse. Four different oscillograms at 4 different oven temperatures (TmI_3 vapor pressures or particle number densities) from 670 °C ($5*10^{14}$ cm^{-3} TmI_3 density) to 880 °C ($5*10^{16}$ cm^{-3} TmI_3 density) are shown. Note the strong, rapidly rising and falling light signal ("spiking") after current-pulse onset. This spiking behavior does only occur for neutral resonance lines (Tm I resonance lines). It can only be observed within a limited TmI_3 partial pressure range of 0.2–2 mb and for discharge voltages in the range 7–15 kV.

Figure 4 gives a measure of the spiking behavior versus oven temperature (Fig. 4a) and discharge voltage (Fig. 4b) in terms of the ratio of the resonance line signal at the spiking peak to this same signal at current maximum. The spiking is completely absent for Tm I transitions between excited levels and also for Tm II ionic lines.

Figure 5 gives a comparison of oscillograms (current i, light signal I) for 3 different Tm I resonance lines and

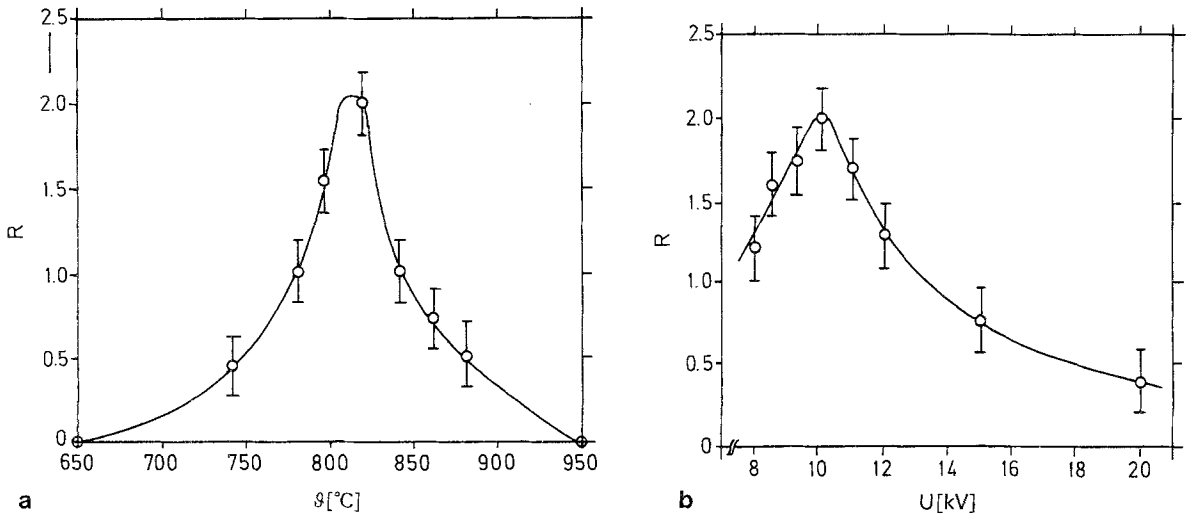

Fig. 4a and b. "Spiking" ratio R versus oven temperature (a) and versus discharge voltage (b). R is the ratio of the light signal at the spiking peak and the light signal at current maximum for $\lambda = 371.8$ nm. (Discharge parameters: $p_{Ar} = 40$ mb, $C_E = 6.6$ nF)

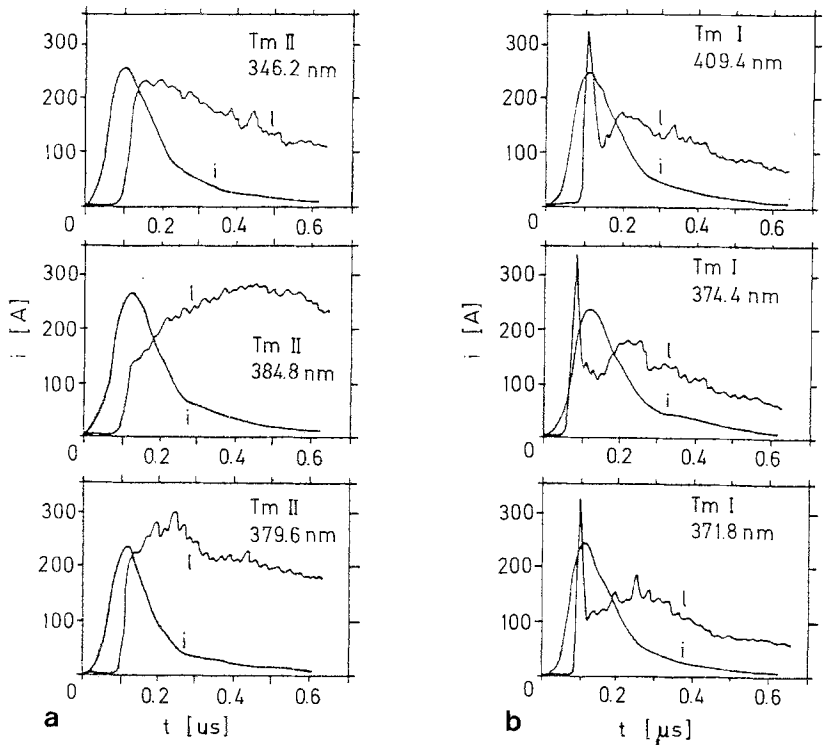

Fig. 5a and b. Comparison of oscillograms of current i and light signal I for 3 different Tm II lines (a) and 3 different Tm I resonance lines (b). (Discharge parameters: $U_C = 10$ kV, $C_E = 6.6$ nF, $p_{Ar} = 40$ mb, $T_{oven} = 1000$ K)

for 3 different Tm II resonance lines [Note that the light signals I in Fig. 5 are delayed by approximately 80 ns with respect to the current signals i due to a long optical path (5m), to different electrical cable lengths and to the electron transit time in the photomultiplier tube used (EMI 9816 QB)]. We emphasize that the resonance line spiking was observed at a total of 13 different Tm I resonance lines in the blue and near uv spectral range.

The occurance of spiking pulses immediately after current onset (within less than 10 ns), i.e. at still very high values of the electrical field strength, suggests a one-step excitation process of the Tm I resonance levels. A suitable excitation process would be one-step

electron collisional dissociation of TmI_3 molecules directly into Tm *I* resonance levels. The rapid decay of the spiking pulses would then be due to resonance transitions to the Tm *I* ground state, which is still largely unpopulated during this early stage of the discharge, i.e. due to resonance fluorescence and induced emission processes in the absence of any appreciable ground state population. It is the rapid decay of the spiking pulse that suggests the existence of population inversion of the resonance lines. With an appreciable ground state population present (in the order of magnitude of the TmI_3 particle number density) substantial afterglow due to radiation trapping is expected instead of the observed rapid decay of the spiking pulse. This afterglow can indeed be seen in the later stages of the above shown oscillograms, i.e. after the decay of the spiking pulses, when a substantial Tm *I* ground-state density has been able to build up. This conclusion is, indeed, proved by a double pulse experiment, where two successive pulses with variable time delay from 20–200 μs are discharged.

Figure 6 shows the resulting oscillograms (current *i*, resonance line signal *I*) for the second discharge pulses. With a time delay $t_d = 25$ μs (upper oscillogram) no resonance line spiking is observed, while resonance line spiking occurs again at $t_d = 100$ μs (lower oscillograms). This behavior is obviously due to the fact that the Tm *I* ground state population, created by the first discharge pulse, is still present after 25 μs and inhibits the creation of population inversion by electron collisional dissociation at the early stage of the second pulse. This is why only resonance fluorescence with strong afterglow due to radiation trapping can be observed. However, at $t_d = 100$ μs, the Tm *I* ground state population seems to have dropped sufficiently due to collisional recombination with iodine atoms and/or molecules and spiking due to inversion of the resonance transition by electron collisional dissociation into the Tm resonance levels does occur again.

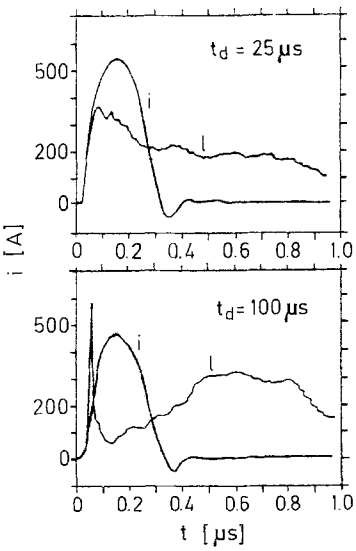

Fig. 6. Oscillograms of second pulses of the double pulse experiment for 2 different delay times $t_d = 25$ μs (top) and $t_d = 100$ μs (bottom). Discharge parameters are: $C_E = 6.6$ nF, $p_{Ar} = 40$ mb, $T_{oven} = 1000$ K, $\hat{i}_1 = 20$ A (first pulse) and $\hat{i}_2 = 500$ A (second pulse)

Discussion

Our experimental results indicate that fast discharges with tens of nanoseconds current rise time in Ar/TmI_3 mixtures produce transient population inversion of a large number of Tm *I* resonance lines. The suggested pumping process is direct electron collisional dissociation of TmI_3 molecules into the neutral Tm resonance levels. For a rough model calculation of such an inversion process, Fig. 7 shows a schematic 3-level diagram of relevant excitation and deexcitation processes. Our calculation assumes the $\lambda = 371.8$ nm resonance line as an example. With n_i as population number densities of the levels *i*, X_{ik} as electron collisional excitation rates from level *i* to level *k*, Y_{ki} as the corresponding electron collisional deexcitation rate and A_{ki} as spontaneous transition probability of level *k* into level *i*, the rate equations used are as follows:

$$dn_0/dt = -n_0(X_{01} + X_{03}), \tag{1}$$

$$dn_1/dt = n_0 X_{01} + n_3(Y_{31} + A_{31}) - n_1 X_{13} + \tilde{P}_{31}, \tag{2}$$

$$dn_3/dt = n_0 X_{03} - n_3(Y_{31} + A_{31}) - \tilde{P}_{31}. \tag{3}$$

$\tilde{P}_{31}$ is the induced net emission rate (minus absorption rate) on the resonance transition. Molecular recombination rates Y_{k0} have been neglected on the time scale of interest to us (first 50 ns after dicharge initiation),

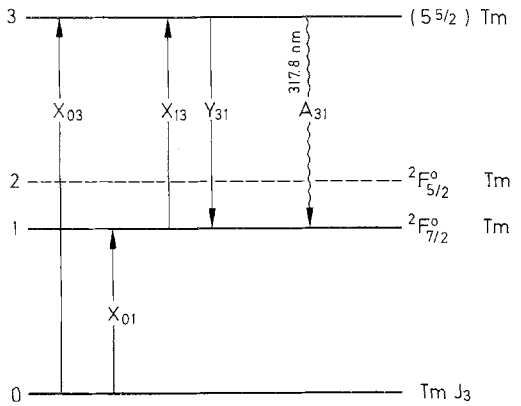

Fig. 7. Schematic level diagram of excitation and deexcitation processes for electron collisional dissociation of TmI_3 into Tm *I* resonance levels

because their relaxation time is in the microsecond time range (see our double pulse experiment). These rate equations are solved for the two limiting cases $\tilde{P}_{31}=0$ (small signal case) and $\Delta n_{31}=n_3-n_1 g_3/g_1=0$ (saturation case) [9]. The first of these solutions yields the resonance line inversion density $\Delta n_{31}(t)$.

Due to the lack of even approximate atomic and molecular data for the TmI_3/Tm-system, we estimated them. For the dissociation energy of TmI_3 we take a typical value for trivalent metal iodides [10] of $E_D=6$ eV. The resonance levels of the observed lines are $E_R=3-4$ eV above the neutral Tm ground level. This yields an excitation threshold (Fig. 7) $E_{03}=9$–10 eV. For an estimate of the electron collisional dissociation rate X_{03} we take a cross-section above threshold of $\sigma_{03}=5*10^{-17}\,\mathrm{cm}^2$ and for the corresponding cross section σ_{01} into the Tm *I* ground state we estimate a value which is 1–2 orders of magnitude smaller. These estimates are based on experience with other molecules like TlI and CuI [10, 11]. The resonance line 371.8 nm, considered in our calculation, has a transition probability $A_{31}=1.35*10^7\,\mathrm{s}^{-1}$ [12]. Using a semiempirical relation from [13], electron collisional excitation and deexcitation crossections σ_{13} and σ_{31} can be estimated from A_{31} and thus the excitation and deexcitation rates X_{13} and Y_{31}, respectively, (Fig. 7) can be calculated.

For a numerical calculation of the rates X_{ik} and Y_{ki}, the relevant plasma parameters of our discharges are required. As we are only interested in the first few tens of nanoseconds, i.e. when we observed spiking, the electron temperature T_e and electron density n_e have to be known for these early times only. Discharge voltage measurements yielded E/n_{Ar} – values from which the electron temperature T_e can be derived from the $T_e=f(E/n_{\mathrm{Ar}})$ relationship for argon discharges. By adding minute quantities of hydrogen to our discharges, we measured the electron density n_e from the Stark broadening of the first 3 Balmer lines [14]. Typical plasma parameters for our discharges, derived from those measurements for the first 30 ns after discharge initiation, are:

$$\text{electron temperatures } T_e=5\text{–}6\,\mathrm{eV}, \tag{4}$$

$$\text{electron density } n_e=10^{14}-10^{15}\,\mathrm{cm}^{-3}, \tag{5}$$

$$\text{rate of electron density rise } \alpha_e=10^{21}-10^{22}\,\mathrm{cm}^{-3}\,\mathrm{s}^{-1}. \tag{6}$$

These parameters yield the following process rates for the case of the Tm *I* 371.8 nm resonance line

$$X_{03}=10^5-10^6\,\mathrm{s}^{-1}, \tag{7}$$

$$X_{01}=10^4-10^5\,\mathrm{s}^{-1}, \tag{8}$$

$$X_{13}=5\times10^6-5\times10^7\,\mathrm{s}^{-1}, \tag{9}$$

$$Y_{31}=8\times10^6-8\times10^7\,s^{-1}. \tag{10}$$

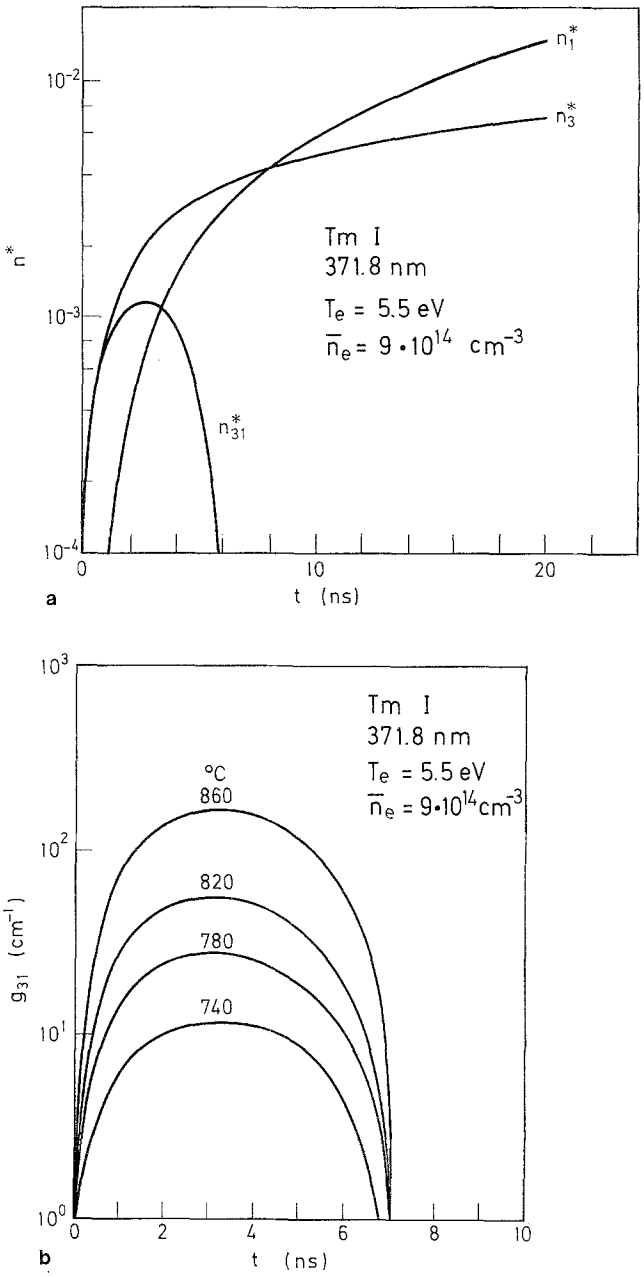

Fig. 8a and b. Time history of Tm *I* level population densities n_1^* and n_3^*, and resonance line inversion density n_{31}^* (a) and small signal gain coefficient g_{31} for the Tm *I* resonance line 371.8 nm (b) for different oven temperatures

Figure 8a shows the calculated time development of the Tm *I* ground and resonance level populations n_1 and n_3 ($n_i=n_{\mathrm{TmI_3}}*n_i^*$) and of the inversion density $\Delta n_{31}(\Delta n_{31}=n_{\mathrm{TmI_3}}*n_{31}^*)$ for the $\lambda=371.8$ nm resonance line during the first 20 ns after discharge initiation. The spiking behavior of the inversion density can be seen clearly, lasting only a few nanoseconds. Figure 8b shows the corresponding small-signal gain coefficient

curves for different TmI_3 vapor pressures (oven temperatures). As the diameter of our discharge plasma is only a few millimeters, the theoretical gain $(g_{31} \times l)$ in the temperature range 780–820 °C, where spiking was observed experimentally, is of the order $(g_{31} \times l) \approx 5$–10. This is still below the threshold for ASE (amplified spontaneous emission), which is assumed empirically at $(g_{31} \times l) \approx 30$ and would explain why we did observe spiking, but did not see any indication of ASE on any resonance line. For temperatures beyond 820 °C we could no longer observe spiking, contrary to the calculated results in Fig. 8b. A possible explanation for this discrepancy is a decrease of electron temperature in the Ar/TmI_3 discharge at higher molecular densities compared to a pure argon or low TmI_3 additive argon plasma due to an increased rate of inelastic electron collisions with TmI_3 molecules. Gain measurements with a modified longitudinal discharge configuration are in progress but have not yet been successful.

Summary

Strong spiking behavior of a large number of thulium resonance lines has been observed in fast discharges through Ar/TmI_3-mixtures during current rise immediatly after discharge initiation. The dynamical behavior of the resonance line emission in both single and double pulse discharges suggests the existence of transient population inversion of these resonance transitions, despite the fact that amplified spontaneous emission (ASE) was not observed. The pumping process is selective electron collisional dissociation of TmI_3 molecules by fast discharge electrons. Results of a rough model calculation of this novel inversion process for resonance lines support our experimental findings, including the absence of ASE in our particular discharge configuration.

References

1. R. Green, J. Travis, R. Keller: Anal. Chem. **48**, 1954 (1976)
2. D.J. Ehrlich, R.M. Osgood, Jr.: IEEE J. QE-**16**, 257 (1980)
3. P. Burckhardt, W. Lüthy, T. Gerber: Opt. Lett. **5**, 522 (1980) R. Schmiele, W. Lüthy, P.-D. Henchoz, H.-P. Weber: Appl. Phys. B**29**, 201 (1982)
4. S. Shadin, K. Ludewigt, B. Wellegehausen: IEEE J. QE-**17**, 1276 (1981)
5. E.J. Schimitschek, J.E. Celto: Opt. Lett. **2**, 64 (1978)
6. J.G. Eden et al.: Appl. Phys. Lett. **43**, 418 (1983)
7. R. Reisfeld, C.K. Jorgensen: *Lasers and Excited States in Rare Earth Elements* (Springer, Berlin, Heidelberg 1977)
8. L.L. Quill: *The Chemistry and Metallurgy of Miscellaneous Materials*, (McGraw Hill, New York 1950)
9. W. Kaesler: "Inversion von Resonanzlinien durch Elektronenstoß-Dissoziation", Dissertation, University of Karlsruhe (1983)
10. T.F. Deutsch, D.J. Ehrlich: Opt. Lett. **4**, 378 (1979)
11. C.S. Liu, L. Weaver et al.: IEEE J. QE-**10**, 190 (1974)
12. K.B. Blagoev, V.A. Komerovski, N.P. Penkin: Opt. and Spectr. **44**, 130 (1978)
13. J. Maya: IEEE J. QE-**15**, 579 (1979)
14. R. Hoppstock: Private communication of unpublished work (1984)